JCB Report

A requirement for MAP kinase in the assembly and maintenance of the mitotic spindle

Melinda M. Horne and Thomas M. Guadagno

Department of Interdisciplinary Oncology, H. Lee Moffitt Comprehensive Cancer Center, and Department of Biochemistry and Molecular Biology, University of South Florida, Tampa, FL 33612

Circumstantial evidence has suggested the possibility of microtubule-associated protein (MAP) kinase's involvement in spindle regulation. To test this directly, we asked whether MAP kinase was required for spindle assembly in *Xenopus* egg extracts. Either the inhibition or the depletion of endogenous p42 MAP kinase resulted in defective spindle structures resembling asters or half-spindles. Likewise, an increase in the length and polymerization of microtubules was measured in aster assays suggesting a role for MAP kinase in regulating microtubule dynamics. Consistent with this, treatment of extracts with either a specific MAP kinase kinase inhibitor or a MAP kinase phosphatase resulted in the rapid disassembly of bipolar spindles into large asters. Finally, we report that mitotic progression in the absence of MAP kinase signaling led to multiple spindle abnormalities in NIH 3T3 cells. We therefore propose that MAP kinase is a key regulator of the mitotic spindle.

Introduction

The mitotic spindle is a dynamic bipolar structure that facilitates chromosome segregation. Regulation of its assembly requires coordinated changes in microtubule dynamics coupled with the mechanical forces generated by microtubule-based motor proteins (for review see Karsenti and Vernos, 2001; Wittmann et al., 2001). These changes are regulated by the action of multiple upstream signaling factors. For example, the Ran signaling network (Dasso, 2001; Walczak, 2001) and many mitotic protein kinases (i.e., Cdc2, Polo-like kinase, Aurora) have been implicated in spindle regulation (Nigg, 2001). Although the mechanisms for these signaling pathways are poorly understood, it is likely that they mediate spindle regulation through regulating microtubule-based regulators such as microtubule-associated proteins (MAPs),* microtubule-destabilizing factors, and motor kinesin-like proteins.

The Mos/MAP kinase kinase (Mek)/MAP kinase cascade is implicated in regulating the meiotic spindle during oocyte maturation (Verlhac et al., 1996). During the mitotic cell cycle, activation of MAP kinase (also known as extracellular signal-regulated kinase [ERK]) has been reported to regulate mitotic progression (Guadagno and Ferrell, 1998; Roberts et al., 2002) and microtubule dynamics (Gotoh et al., 1991; Guadagno and Ferrell, 1998). Consistent with a role in regulating the mitotic spindle, active forms of ERK1/2 are observed from prophase to anaphase at the spindle poles, spindle microtubules, kinetochores, and during cytokinesis at the midbody (Shapiro et al., 1998; Zecevic et al., 1998). Collectively, a picture has emerged suggesting the involvement of MAP kinase signaling in regulating the mitotic spindle. However, evidence directly supporting this possibility has been lacking.

Results and discussion

Active MAP kinase is required for spindle assembly in *Xenopus* egg extracts

We exploited *Xenopus* egg extracts to reconstitute spindle assembly and asked whether MAP kinase signaling was required. To do this, *Xenopus* egg extracts containing duplicated sperm chromosomes were cycled into metaphase in the presence or absence of the pharmacological MEK inhibitor U0126. U0126 inhibits MEK1/2 and not other MAP kinase family members or related kinases (Davies et al., 2000). As expected, the addition of 50 μM U0126 strongly inhibited MAP kinase activation but had no detectable effect on either Cdc2 or a related MAP kinase family member, JNK1 (Fig. 1 A). Next, spindle assembly was monitored in control- and

Address correspondence to Thomas M. Guadagno, H. Lee Moffitt Cancer Center & Research Institute, Building MRC 3 annex, 12902 Magnolia Drive, Tampa, FL 33612. Tel.: (813) 903-6818. Fax: (813) 903-6817. E-mail: guadagnt@moffitt.usf.edu

*Abbreviations used in this paper: CSF, cytostatic factor; ERK, extracellular signal-regulated kinase; MAP, microtubule-associated protein; Mek, MAP kinase kinase; MKP-1, MAP kinase phosphatase-1; Rsk, ribosomal S6 kinase; UO126, 1,4-diamino-2,3-dicyano-1,4-bis(2-aminophenylthio)butadiene.

Key words: MAP kinase; Rsk; spindle assembly; *Xenopus*; mitotic spindle

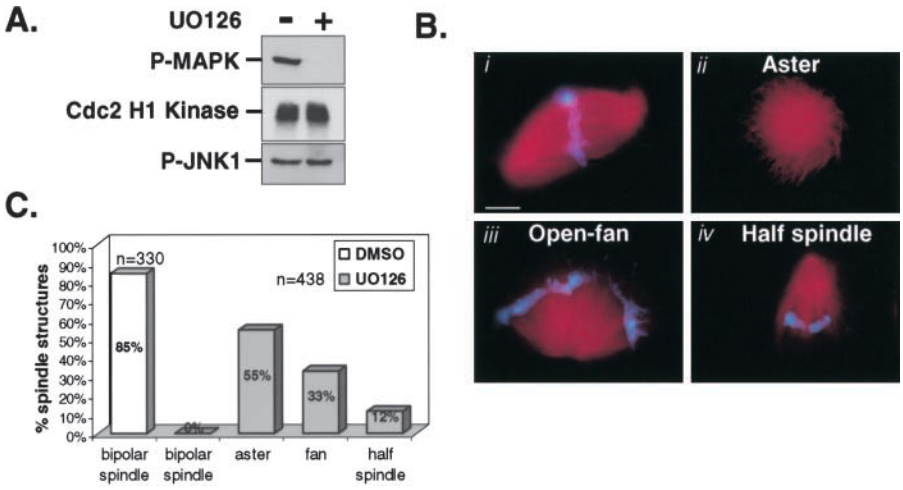

Figure 1. **The MEK inhibitor UO126 blocks spindle assembly in *Xenopus* mitotic egg extracts.** Spindle assembly reactions were assessed in the presence of 50 μM U0126 or 0.5% DMSO. Aliquots of extract were collected at 75 min for (A) biochemical analysis of active MAP kinase (p-MAP kinase), Cdc2 H1 kinase activity, and active JNK1 (p-JNK1); (B) monitoring spindle structures formed in control- (0.5% DMSO) (i) and UO126-treated extracts (ii, iii, and iv); and (C) quantitation of spindle structures in DMSO- and U0126-treated extracts. Results are representative of at least three independent experiments. Note: spindle assembly was never observed in U0126-treated extracts monitored at 10-min intervals from 30–120 min. Cdc2 H1 kinase assays were performed as described (Guadagno and Ferrell, 1998). Bar, 10 μm.

U0126-treated extracts by epifluorescence. By 60–75 min, metaphase spindles were formed in control extracts (Fig. 1 B, i, and 1 C). In contrast, the assembly of metaphase spindles was completely blocked in the absence of MAP kinase activation (Fig. 1 B, ii, iii, and iv). Typically, we observed three defective spindle phenotypes in U0126-treated extracts: monastral structures without condensed chromatin, open fan-like microtubule structures that are loosely associated with unorganized condensed chromatin, and half-spindle–like structures containing compact chromatin bodies. The relative percentage for each of these phenotypes is shown in Fig. 1 C.

Our data in Fig. 1 suggest that MAP kinase activation is important for spindle assembly. To test this further, we depleted endogenous MAP kinase from CSF-arrested egg extracts using *Xenopus*-specific MAP kinase antibodies. After two rounds of immunodepletion, immunoblot analysis showed that MAP kinase was quantitatively removed (~97%) from CSF-arrested egg extracts (Fig. 2 A). Spindle assemble reactions were initiated in both mock- and MAP kinase–depleted extracts supplemented with sperm DNA, rhodamine-labeled tubulin, and nondegradable cyclin B. Spindle assembly was observed in mock-depleted extracts (Fig. 2 C, left), although at a slightly lower efficiency

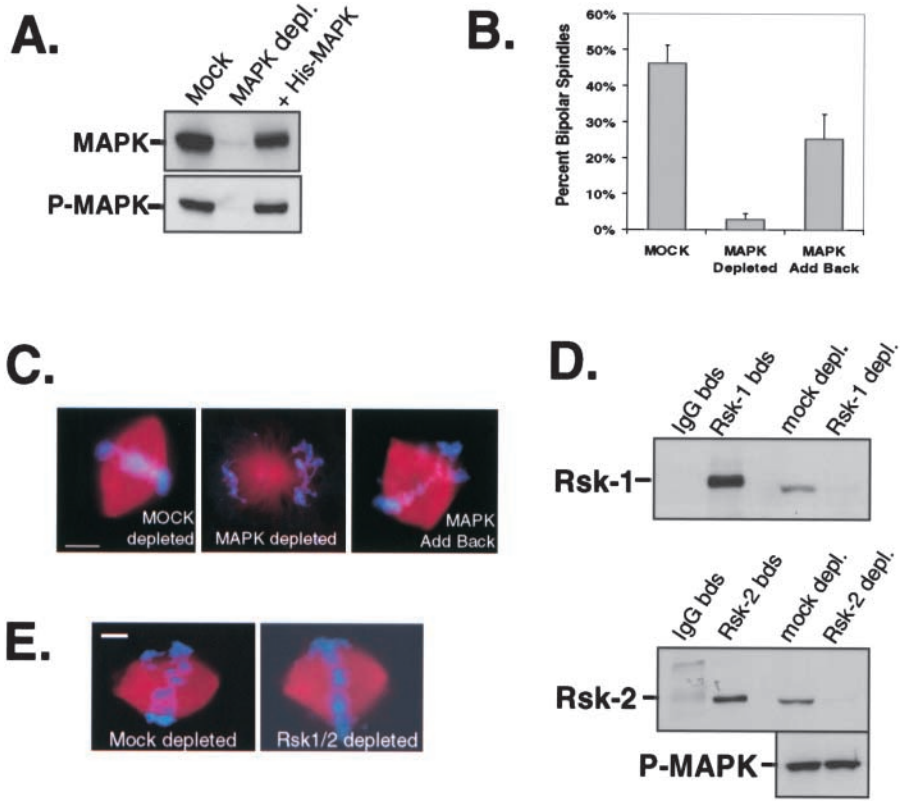

Figure 2. **MAP kinase, not Rsk, is required for spindle assembly in *Xenopus* egg extracts.** (A) Immunoblot analysis of endogenous MAP kinase protein and activity (p-MAPK antibody). (B) The efficiency of spindle assembly. 500 spindle structures were counted per sample. The data represent the average ± SEM obtained from three independent experiments. (C) Representative spindle structures. Bar, 10 μm. (D) immunoblots of Rsk1 and Rsk2. (E) Metaphase spindles assembled in mock- and Rsk1/2-depleted extracts. Bar, 10 μm. From three independent experiments the efficiency of spindle formation was ~50% in mock- and Rsk1/2-depleted extracts (>100 spindle structures assessed per extract). Note: no statistical difference in microtubule density, spindle length, and spindle width was found between spindles formed in mock- or Rsk-depleted extracts (unpublished data).

Table I. **Summary of the effects of MAPK immunodepletion on microtubule aster formation**

Extract	Total fluorescence intensity	Average fluorescence intensity	Radius
	arbitrary units	*arbitrary units*	*μm*
Experiment 1			
MOCK depleted	1.08 ± 0.17	536 ± 83.0	6.81 ± 1.13
MAPK depleted	1.42 ± 0.20	735 ± 101	8.42 ± 1.16
His-MAPK add back	0.86 ± 0.21	430 ± 105	6.23 ± 1.19
Experiment 2			
MOCK depleted	1.18 ± 0.37	587 ± 184	7.70 ± 1.94
MAPK depleted	1.50 ± 0.35	747 ± 175	9.19 ± 1.40
His-MAPK add back	0.78 ± 0.26	386 ± 128	6.01 ± 1.44
Experiment 3			
MOCK depleted	1.62 ± 0.42	810 ± 209	8.21 ± 0.63
MAPK depleted	2.23 ± 0.39	1111 ± 195	10.50 ± 0.89
His-MAPK add back	1.01 ± 0.28	502 ± 139	6.05 ± 1.10
Average			
MOCK depleted	1.31 ± 0.41	651 ± 204	7.44 ± 1.42
MAPK depleted	1.70 ± 0.46	848 ± 227	9.25 ± 1.34
His-MAPK add back	0.88 ± 0.26	439 ± 130	6.35 ± 1.30

Values are means ± SEM from three independent experiments. Differences in mean total fluorescence intensity, average fluorescence intensity, and aster radius were significantly different ($P < 0.001$) by the unpaired *t* test. $n > 30$ per sample.

(~45%) than usual due to the two rounds of depletion (Fig. 2 B). However, the efficiency of spindle assembly was strongly inhibited (<3%) in MAP kinase–depleted extracts (Fig. 2 B). In contrast to the multiple spindle defects observed in U0126-treated extracts, there is a strong preference for forming monastral structures in MAP kinase–depleted extracts (Fig. 2 C, middle). We speculate that these differences may be related to how spindle assembly proceeds in CSF-arrested extracts compared with extracts cycled into mitosis. For instance, in extracts that are cycled, the kinetochores and centrosomes are duplicated before spindle assembly, whereas this does not occur in CSF-arrested extracts. As an important control for the immunodepletion of MAP kinase, recombinant $(his)_6$–tagged MAP kinase protein was added back to extracts depleted of MAP kinase. This restored MAP kinase activity (Fig. 2 A, lane 3) and the assembly of metaphase spindles (Fig. 2 B and C, right).

p90 Rsk is not required for spindle assembly in *Xenopus* CSF-arrested egg extracts

Upon activation of the MAP kinase cascade, p90 Rsk is phosphorylated and activated directly by MAP kinase during oocyte maturation (Gross et al., 2000; Kalab et al., 1996) and at mitosis in *Xenopus* egg extracts (Bhatt and Ferrell, 1999). Therefore, we tested whether MAP kinase regulation of spindle assembly was exerted through p90 Rsk. Since two closely related Rsk isoforms, Rsk1 and Rsk2, are present and active in *Xenopus* eggs (Bhatt and Ferrell, 2000), we used specific Rsk1 and Rsk2 antibodies to sequentially immunodeplete both proteins from CSF-arrested egg extracts. As indicated by immunoblot analysis for Rsk1 and Rsk2, both proteins were quantitatively removed (>95%) compared with mock-depleted extracts (Fig. 2 D) without affecting endogenous levels of active MAP kinase (Fig. 2 D) or Cdc2 activity (data not shown). Interestingly, in the absence of p90 Rsk, spindle assembly was not compromised (Fig. 2 E): both spindle appearance and the efficiency of spindle formation were similar in mock- and Rsk1/2-depleted extracts (see Fig. 2 legend). Thus, we conclude that p42 MAP kinase, not p90 Rsk, is required for directly regulating spindle assembly in *Xenopus* egg extracts.

Depletion of p42 MAP kinase leads to an increase in the length and polymerization of microtubules in *Xenopus* M phase egg extracts

Contrary to the static appearance of bipolar spindles, spindle microtubules are very dynamic with a turnover rate of 60–90 s (Saxton et al., 1984). Therefore, we asked whether MAP kinase might play a role in regulating microtubule dynamics. To address this, we immunodepleted endogenous p42 MAP kinase (~96%) from CSF-arrested egg extracts (Fig. 3 A) and measured the length and polymerization of microtubules using an aster assay. As evident in Fig. 3 B, microtubule asters were markedly larger in CSF-arrested extracts depleted of MAP kinase compared with mock-depleted extracts. Precisely, a 24% increase in mean aster radius was measured over three independent experiments (Table I). Furthermore, the average total fluorescence intensity/aster increased 30% in MAP kinase–depleted extracts compared with mock-depleted extracts, indicative of an increase in microtubule polymerization (Table I). Consistent with this, an increase in tubulin was observed in pelleted microtubules from CSF-arrested extracts depleted of MAP kinase activity (Fig. 3 C). Importantly, the addition of recombinant $(his)_6$-tagged MAP kinase protein to depleted extracts restored MAP kinase activity (Fig. 3 A) and rescued the effects on microtubule polymerization and microtubule length (Fig. 3, B and C, and Table I). Together, our data support a role for MAP kinase in regulating microtubule dynamics. Further analysis will be required to precisely define which of the parameters of microtubule dynamics are regulated by MAP kinase.

Spindle stability requires active MAP kinase

Consistent with reports in tissue culture cells (Shapiro et al., 1998; Zecevic et al., 1998), we observed active forms of

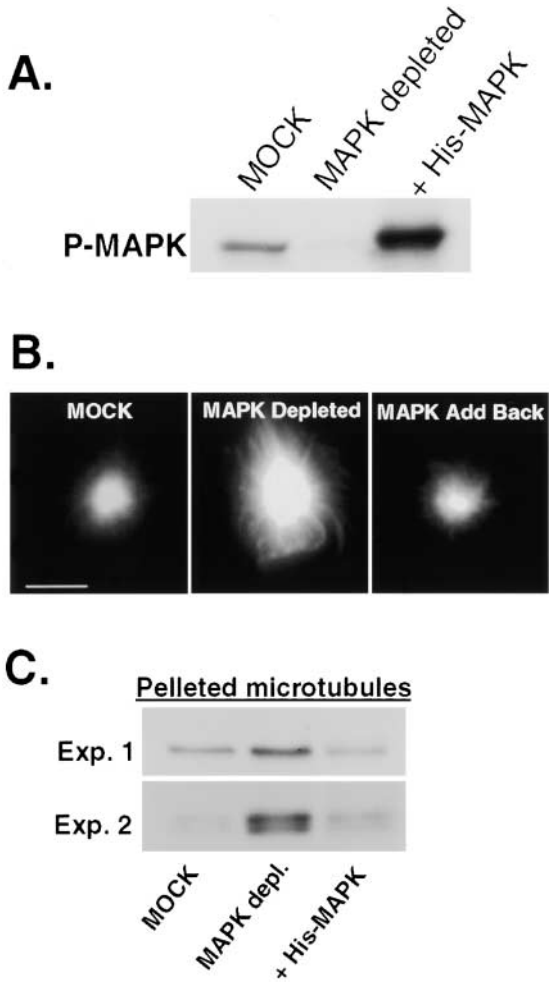

Figure 3. **Depletion MAP kinase in *Xenopus* M phase egg extracts leads to an increase in the length and polymerization of microtubules.** (A) Immunoblot of phospho-MAP kinase. Reprobing the blot for MAP kinase protein shows similar results. (B) Typical microtubule asters. Bar, 10 μM. (C) Immunoblots of α-tubulin for two independent experiments representing the relative abundance of polymerized microtubules in mock, MAP kinase–depleted, and MAP kinase add-back extracts. A two- to sixfold increase in total polymerized tubulin was measured in MAP kinase–depleted extracts.

MAP kinase on metaphase spindles reconstituted in *Xenopus* mitotic egg extracts (Fig. 4 A). Since spindle microtubules are very dynamic, it stands to reason that interfering with MAP kinase activation might lead to the destabilization of the bipolar spindle structure. To test this possibility, we first assembled metaphase spindles in *Xenopus* egg extracts cycled into mitosis in the presence of nondegradable cyclin B and rhodamine-labeled tubulin. Then, MAP kinase was inactivated by treating the extract with either UO126 or recombinant *Xenopus* MAP kinase phosphatase-1 (MKP-1). Aliquots of extract were collected at 20-min intervals and analyzed for MAP kinase inactivation and spindle stability. Coincident with MAP kinase inactivation (Fig. 4 B), >95% of the bipolar spindles had disassembled and by 40 and 60 min converted to large aster-like structures (Fig. 4 C). Moreover, we observed a dispersion of mitotic chromatin from the spindle microtubules, suggesting a role for MAP kinase in maintaining spindle–chromosome interactions. In contrast, bipolar spindles remained stable in control extracts for the duration of the experiment (≥90 min). Thus, despite the continued presence of Cdc2 activity, spindle stability appears to also require the persistent activation of MAP kinase.

ERK inhibition leads to numerous spindle abnormalities in tissue culture cells

We asked whether ERK1/2 signaling might play a similar role during mitosis in somatic cells by treating G2 phase synchronized mouse NIH 3T3 cells with the MEK inhibitor U0126 (Fig. 5 A). ERK1/2 activity, as measured by immunoblotting with phospho-specific MAP kinase antibodies, was nearly undetectable in cells treated with 30 μM UO126 compared with controls (Fig. 5 B). Previous studies have shown a role for MAP kinase in cell cycle progression at the G2/M transition (Wright et al., 1999). Consistent with these studies, when we treated NIH 3T3 cells earlier at S phase with the MEK inhibitor, we observed a partial G2 phase delay. However, the addition of the MEK inhibitor to cells synchronized at late G2 had little affect on entry into mitosis as measured by the mitotic index (unpublished data).

To assess the role of ERK1/2 signaling on spindle regulation, NIH 3T3 cells were plated onto glass coverslips in dishes and treated in parallel with 30 μM U0126. Following a 2–3-h treatment, the mitotic-enriched cells were fixed with 4% paraformaldehyde and immunostained for microtubules with α-tubulin antibodies. DAPI was used to stain the DNA (blue) for identifying chromosomes and the phase of mitosis. As expected, normal mitotic figures were observed in control-treated cells, indicating that 0.5% DMSO alone does not perturb spindle regulation (Fig. 5 C, left). In contrast, 35–45% of the mitotic figures in U0126-treated cells showed aberrant spindles and misaligned chromosomes. Examples of abnormal spindle phenotypes are shown in Fig. 5 C. Densely stained aster-like structures surrounded by unorganized chromosomes comprise 65% of the spindle abnormalities (Fig. 5 D). Also prevalent are metaphase-like spindles with variable defects in chromosome alignment (MAPK-inhibited; Fig. 5 C, bottom-left). The remaining percent of mitotic defects represent abnormal chromosome segregation during anaphase/telophase or multipolar (>2 poles) spindles (Fig. 5 D). It is noteworthy that similar spindle abnormalities were observed when primary human foreskin fibroblast (HFF) cells were treated with U0126 or when NIH 3T3 cells were treated with a different MEK inhibitor, PD098059 (unpublished data). Collectively, these results are consistent with our data in *Xenopus* egg extracts and indicate that ERK1/2 signaling is critical for mediating spindle regulation in mammalian cells.

Since its early discovery as a microtubule-associated protein kinase (Ray and Sturgill, 1987; Reszka et al., 1995), MAP kinase has been suspected of regulating microtubules. Our data provide the first biochemical evidence that directly demonstrates a requirement for MAP kinase in the assembly and maintenance of the mitotic spindle. Our data also support a role for MAP kinase in regulating microtubule dynamics (Figs. 3 and 4). Furthermore, our Rsk immunode-

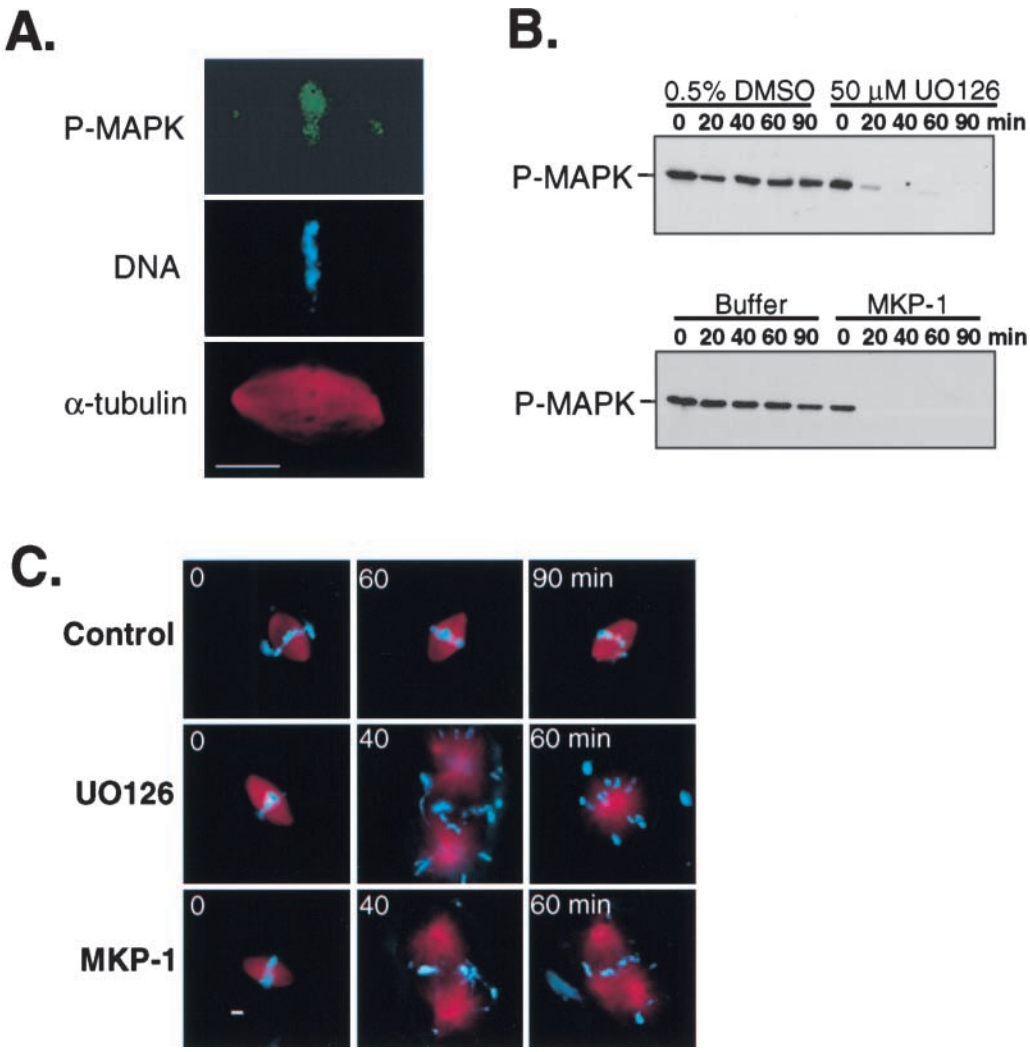

Figure 4. **Spindle stability requires persistent MAP kinase activation in *Xenopus* mitotic extracts.** Bipolar spindles were assembled in *Xenopus* egg extracts cycled into mitosis with nondegradable cyclin B. At time 0, extracts were either processed for immunofluorescence with phospho–MAP kinase antibodies (A), or treated with the MEK inhibitor U0126 (50 μM final) or recombinant *Xenopus* GST-MKP-1 (40 ng/μl final). (B) Immunoblot analysis of active-MAP kinase at indicated time points. (C) Typical spindle or aster-like structures observed by epifluorescence at selected times following treatments. 100 spindle structures monitored for each sample per time point. Bar, 10 μm.

pletion data (Fig. 2) allow us to propose a model through which the Mek/MAP kinase/Rsk cascade bifurcates at MAP kinase and Rsk to elicit separate biological responses during mitosis (see model; Fig. 5 E). In this proposal MAP kinase likely targets spindle regulators (directly or indirectly) by phosphorylation to mediate spindle assembly and stability. Support for this comes from Verlhac and colleagues who have identified two MAP kinase–interacting proteins, MISS (Lefebvre et al., 2002) and DOCR1 (Verlhac, M.-H., personal communication); both proteins are phosphorylated by MAP kinase and appear to be necessary for regulation of the meiotic spindle.

Contrary to our p90 Rsk immunodepletion results (Fig. 2), an active p90 Rsk mutant injected into progesterone-treated *Xenopus* oocytes incubated with U0126 was shown to restore both CSF arrest and spindle formation in the absence of MAP kinase activity (Gross et al., 2000). This discrepancy might reflect differences in the regulation of the meiotic spindle versus the mitotic spindle. Indeed, in our study sperm DNA–associated centrioles are supplemented in the *Xenopus* egg extracts to recapitulate the assembly of the mitotic spindle. Clearly, further studies are required to define the precise roles of MAP kinase and p90 Rsk during meiosis and mitosis. Nevertheless, our data show that depletion of both Rsk1 and Rsk2 has no effect on spindle assembly in the presence of active MAP kinase. Based on Rsk's role as an essential MAP kinase mediator for establishing (but not maintaining) the CSF arrest in unfertilized vertebrate oocytes (Bhatt and Ferrell, 1999; Gross et al., 2000), Rsk activation during mitosis may mediate cell cycle events associated with suppressing the metaphase-to-anaphase transition (Schwab et al., 2001). This implies that MAP kinase and Rsk cooperate in coordinating spindle assembly and mitotic progression.

The complex localization pattern of active MAP kinase at the mitotic spindle (Shapiro et al., 1998; Zecevic et al., 1998; Fig. 4 A) suggests multiple targets are under its regulation. As such, blocking MAP kinase activation would perturb the activity of many downstream components of this pathway.

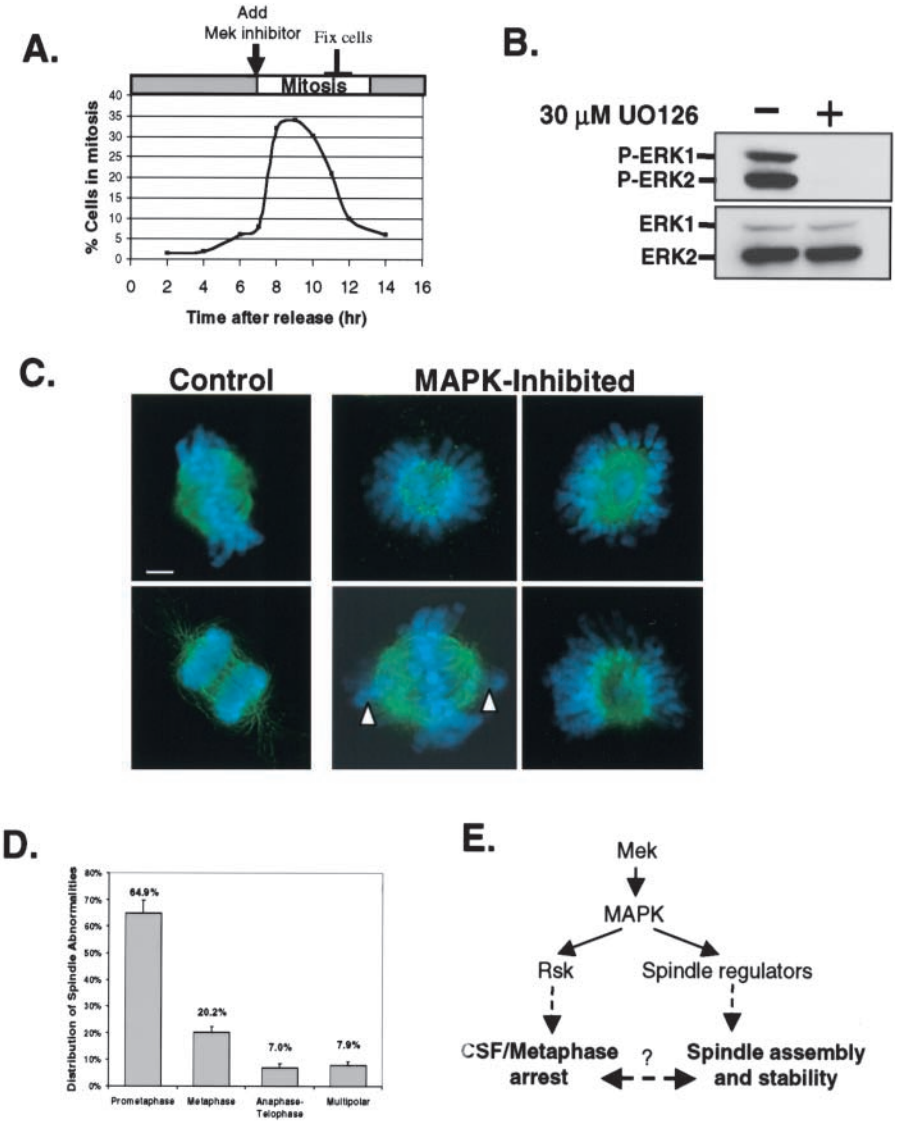

Figure 5. **Inhibition of MAP kinase in NIH 3T3 cells leads to aberrant spindles.** (A) Time course of mitotic index and experimental scheme. Cells collected for immunoblot analysis of active-ERK and total ERK protein (B) or fixed with 4% paraformaldehyde (C) and stained with α-tubulin antibodies and DAPI to visualize spindle microtubules (green) and chromosomes (blue), respectively. (Left) Control-treated cells in metaphase and late anaphase. (Right photos) Abnormal spindles observed in MAP kinase–inhibited cells at mitosis (typical from ten independent experiments). White arrows show unattached chromosomes. Images were collected using a 100X oil objective lens. Bar, 2 μm. (D) Quantitation of abnormal spindle phenotypes in U0126 treated NIH 3T3 cells. The data represent the average ± standard deviation of three independent experiments where 120 abnormal mitotic figures were analyzed for each experiment. (E) Proposed model for MAP kinase pathway in spindle regulation.

These components might include MISS or DOCR1, as well as conventional MAPs, microtubule-destabilizing proteins, and microtubule-based motor proteins. Consistent with this proposal, our studies show multiple spindle abnormalities in the absence of MAP kinase signaling, and this may represent a loss of function of several microtubule regulators. Studies are in progress to identify MAP kinase targets that are linked to its role in regulating the mitotic spindle. Although the regulation of the mitotic spindle by other signaling pathways (i.e., Ran, Cdc2, Plks, and Aurora) has been shown (Nigg, 2001), our data argue that the MAP kinase pathway is an important component of this signaling network.

Materials and methods

Preparation of *Xenopus* egg extracts and spindle assembly

Cytostatic factor (CSF)–arrested extracts prepared from unfertilized *Xenopus* eggs and spindle assembly reactions were preformed as described (Desai et al., 1999), except that for spindle assembly recombinant nondegradable cyclin B (75 nM final) was routinely used to cycle the extracts into mitosis. Extracts cycled with an equal volume of CSF extract also gave similar results. Rhodamine-labeled bovine brain tubulin (Cytoskeleton) was added to a final concentration of 0.15 μg/μl in extracts to visualize microtubules. For immunodepletion experiments, we found it necessary to form half-spindles directly in CSF-arrested egg extracts as described (Desai et al., 1999). To monitor spindles and associated chromosomes, 2 μl of extract and 1 μl of Hoechst/fixative (25% glycerol, 7.4% formaldehyde, 0.1 mM Hepes pH 7.5, 4 μg/ml bisbenzimide) were applied to a microscope slide and examined by epifluorescence.

Aster assays and microtubule pelleting

Microtubule polymerization was stimulated from sperm DNA (250/μl) in fresh CSF-arrested extracts (mock or MAP kinase depleted) for 10 min at 24°C in the presence of rhodamine-labeled tubulin. Microtubule asters were fixed in 0.25% glutaraldehyde solution containing BRB80 (80 mM Pipes, 1 mM EGTA, 1 mM $MgCl_2$, pH 6.8) and 0.5% Triton X-100 for 5 min at 24°C. Alternatively, microtubules were pelleted to assess total polymerized tubulin in extracts. Specifically, 20 μl of extract was diluted into 0.5 ml BRB80/30% glycerol/1% Triton X-100, layered onto a 1-ml BRB80/40% glycerol cushion, and centrifuged for 20 min, 14,000 rpm, at 4°C. The pellet was resuspended in SDS sample buffer, separated by 10% SDS PAGE, and immunoblotted for α-tubulin. Quantification of α-tubulin bands was performed using Image Quant v5.0 software.

Recombinant protein production and purification

pGEX plasmids encoding GST fused to nondegradable sea urchin Δcyclin B1 (missing 13 NH_2-terminal amino acids) or wild-type *Xenopus* MKP-1 (gift from Jim Ferrell and Mike Sohaskey [Stanford University, Stanford, CA]) were transformed into the bacterial strain BL21(DE3), grown in 2 liters LB media to an OD_{595} of 0.6 at 37°C, and induced for

protein expression with 0.2 mM IPTG at 30°C for 3 h. Recombinant GST–Δcyclin B1 was purified from bacterial lysates as previously described (Solomon et al., 1990). Recombinant GST-MKP1 protein was affinity purified on glutathione–sepharose beads as suggested (Amersham Biosciences). A plasmid encoding histidine $(his)_6$-tagged *Xenopus* MAP kinase with a T7 promoter was transformed into BL21(DE3)pLysS, and recombinant fusion protein expressed in the presence of ampicillin (75 μg/ml) and chloramphenicol (35 μg/ml) using similar growth conditions as described above. Recombinant $(his)_6$-tagged MAP kinase proteins were purified using talon metal affinity resin (CLONTECH Laboratories, Inc.). Eluted fractions containing recombinant GST- or $(his)_6$-tagged fusion proteins were concentrated using Centricon 30 concentrators (Amicon Bioseparations) and buffer exchanged with XB buffer (10 mM Hepes, 1 mM $MgCl_2$, 0.1 mM $CaCl_2$, 100 mM KCl, 50 mM sucrose, pH 7.7, with KOH).

Immunodepletions

p42 MAP kinase was removed from CSF-arrested egg extracts by two rounds of immunodepletion as follows: protein A–purified anti-MAP kinase antibodies (X-15 serum kindly provided by Jim Ferrell) were prebound to 10-μl packed protein A–Sepharose 4B fast flow beads (Sigma-Aldrich), washed twice with 20 volumes of XB buffer, and incubated with 60 μl of fresh CSF-arrested egg extract for 45–60 min on ice with occasional mixing. Then, the antibody–bead complexes were pelleted for 15 s in an Eppendorf centrifuge. The MAP kinase–depleted extract was carefully removed and subjected to one more round of depletion. Rsk1 and Rsk2 depletions were performed sequentially using polyclonal rabbit Rsk1 and goat p90 Rsk2 antibodies (Santa Cruz Biotechnology, Inc.), respectively. Mock-depletions were performed using affinity-purified whole molecule anti–rabbit IgG (Sigma-Aldrich). To analyze Rsk proteins bound to the beads, the antibody–bead complexes were washed three times with EB buffer (80 mM β-glycerol phosphate, pH 7.3, 20 mM EGTA, 15 mM $MgCl_2$) containing 0.1% Triton X-100, boiled in SDS-PAGE sample buffer, and subjected to gel electrophoresis.

Cell culture and cell synchronization

NIH 3T3 cells (obtained from American Type Culture Collection) were maintained in DMEM supplemented with 10% calf serum and 46 μg/ml gentamycin. Cells were synchronized at the G1/S boundary using a double-thymidine treatment method as described (Spector et al., 1998). The G1/S-synchronized cells were washed with DMEM and incubated in DMEM containing 10% calf serum to resume cycling into S, G2, and M phase. Cell synchronization was monitored by FACS analysis of DNA content (performed by H. Lee Moffitt Cancer Center Flow cytometry core facility). The mitotic index was determined hourly by analyzing at least 200 cells using a Nikon phase–contrast inverted microscope.

Immunostaining of mitotic spindles

Xenopus egg extract (25 μl) containing rhodamine-labeled spindles was diluted 1:10 in BRB80/0.5% Triton X-100/0.25% glutaraldehyde and fixed for 5 min at room temperature. The fixed spindles were layered on a 5-ml BRB80/20% glycerol cushion and centrifuged onto 12-mm glass coverslips in a HB-6 rotor at 6,000 RPM for 22 min at 4°C. Following the aspiration of the supernatant, the coverslips were gently rinsed twice with 5 ml of BRB80 buffer and postfixed with –20°C methanol for 5 min. Spindles were subjected to indirect immunofluorescence with antiphospho–MAP kinase antibodies (Cell Signaling) diluted 1:100 in Tris-buffered saline (10 mM Tris, pH 7.4, and 150 mM NaCl) containing 2% BSA and 0.1% Triton X-100. Phospho-MAP kinase staining was detected with Alexa Fluor 488 goat anti–rabbit IgG (Molecular Probes) secondary antibodies. DNA was stained with 1 μg/ml Hoechst in PBS. NIH 3T3 cells grown on glass coverslips were fixed in 4% paraformaldehyde (EM Sciences) at 4°C for 20 min, permeabilized for 1 h with 0.5% Triton X-100 in PBS, and labeled with anti–α-tubulin (Sigma-Aldrich, clone B-5–1-2) and Alexa Fluor 488 goat anti–mouse IgG secondary (Molecular Probes) antibodies to detect microtubule spindles. Antibodies were diluted in PBS/0.1% Triton X-100 containing 2% BSA and incubated for 1 h at room temperature. Three washes were performed with PBS/0.1% Triton X-100. Slides were mounted with Vectashield mounting medium containing DAPI (Vector Laboratories) to stain chromosomes.

Fluorescence imaging

Fluorescent images were captured by a Roper coolsnap HQ CCD camera mounted on a Nikon E800 fluorescence microscope and controlled by Metamorph software v5.0r1 (Universal Imaging Corp.). Image processing was performed using Metamorph and Adobe Photoshop 6.0 software.

Immunoblotting analysis

NIH 3T3 cells grown on 100-mm dishes were collected in ice-cold 1X PBS, pelleted by centrifugation, and lysed in cell lysis buffer (50 mM Tris-HCl, pH 7.5, 100 mM NaCl, 1% Triton X-100, 5 mM EDTA, 50 mM sodium fluoride, 200 μM sodium vanadate, 40 mM β-glycerophosphate) supplemented with fresh protease inhibitors (100 μM PMSF; 1 μg/ml each of leupeptin, pepstatin A, and aprotinin). Cell lysates were centrifuged for 10 min at 4°C at 14,000 *g*. Clarified supernatants were transferred to new tubes, and protein concentrations were determined by standard Bio-Rad Laboratories protein assays. 50 μg of protein from NIH 3T3 cell lysates or 25 μg of protein from *Xenopus* egg extracts was separated by 10% SDS-PAGE, electrotransferred onto Immobilon-P membranes, and examined by immunoblot analysis. Antibodies used include rabbit polyclonal anti–*Xenopus* MAP kinase peptide antibody X-15 or a similar one prepared in our laboratory, goat-polyclonal Rsk2 antibodies (Santa Cruz Biotechnology, Inc.), rabbit polyclonal Rsk1 antibodies (Santa Cruz Biotechnology, Inc.), p44/42 Phospho-MAP kinase monoclonal antibody (Cell Signaling), and phospho-JNK-1 (G-7) monoclonal (Santa Cruz Biotechnology, Inc.). A rabbit polyclonal Erk2 antibody (Transduction Laboratories) was used to detect total Erk protein in NIH 3T3 cell lysates. Species-specific alkaline phosphatase–conjugated secondary IgG antibodies were obtained from Jackson ImmunoResearch Laboratories. Antibodies were diluted in 5% dry milk in PBS/0.1% Tween 20 and incubated for 1 h at room temperature or, in the case for p44/42 phospho-MAP kinase monoclonal antibody, incubated overnight at 4°C. To visualize protein bands, blots were incubated for 5 min with CDP-Star chemiluminescence substrate (Roche Diagnostic) and exposed to Kodak Biomax MS film.

We thank Jim Ferrell, Natalie Ahn (University of Colorado at Boulder, Boulder, CO), and Said Sebti (Moffitt Cancer Center, Tampa, FL) for plasmids and antibodies; Yanfen Chen for her valuable technical assistance; Luke Macyszyn and Nichole Crespo for their early contributions to these studies; and Marie-Hélène Verlhac for sharing unpublished data. We are grateful to Sally Kornbluth and Michele Pagano for their comments on the manuscript, and for the helpful feedback from members of the H. Lee Moffitt Cancer Center.

We acknowledge the support of the flow cytometry and analytical microscopy core facilities at the H. Lee Moffitt Cancer Center. This work was supported by the National Institutes of Health (grant GM62542) and a Moffitt institutional award from the American Cancer Society (to T.M. Guadagno). T.M. Guadagno was supported as a Special Fellow of the Leukemia & Lymphoma Society. M.M. Horne is a predoctoral fellow supported by the American Heart Association-Florida division.

Submitted: 25 April 2003
Revised: 14 May 2003
Accepted: 14 May 2003

References

Bhatt, R.R., and J.E. Ferrell, Jr. 1999. The protein kinase p90 rsk as an essential mediator of cytostatic factor activity. *Science.* 286:1362–1365.

Bhatt, R.R., and J.E. Ferrell, Jr. 2000. Cloning and characterization of Xenopus Rsk2, the predominant p90 Rsk isozyme in oocytes and eggs. *J. Biol. Chem.* 275:32983–32990.

Dasso, M. 2001. Running on Ran: nuclear transport and the mitotic spindle. *Cell.* 104:321–324.

Davies, S.P., H. Reddy, M. Caivano, and P. Cohen. 2000. Specificity and mechanism of action of some commonly used protein kinase inhibitors. *Biochem. J.* 351:95–105.

Desai, A., A. Murray, T.J. Mitchison, and C.E. Walczak. 1999. The use of Xenopus egg extracts to study mitotic spindle assembly and function in vitro. *Methods Cell Biol.* 61:385–412.

Gotoh, Y., E. Nishida, S. Matsuda, N. Shiina, H. Kosako, K. Shiokawa, T. Akiyama, K. Ohta, and H. Sakai. 1991. In vitro effects on microtubule dynamics of purified Xenopus M phase-activated MAP kinase. *Nature.* 349:251–254.

Gross, S.D., M.S. Schwab, F.E. Taieb, A.L. Lewellyn, Y.W. Qian, and J.L. Maller. 2000. The critical role of the MAP kinase pathway in meiosis II in Xenopus oocytes is mediated by p90(Rsk). *Curr. Biol.* 10:430–438.

Guadagno, T.M., and J.E. Ferrell, Jr. 1998. Requirement for MAPK activation for normal mitotic progression in Xenopus egg extracts. *Science.* 282:1312–1315.

Kalab, P., J.Z. Kubiak, M.H. Verlhac, W.H. Colledge, and B. Maro. 1996. Activa-

tion of p90rsk during meiotic maturation and first mitosis in mouse oocytes and eggs: MAP kinase-independent and -dependent activation. *Development.* 122:1957–1964.

Karsenti, E., and I. Vernos. 2001. The mitotic spindle: a self-made machine. *Science*. 294:543–547.

Lefebvre, C., M.E. Terret, A. Djiane, P. Rassinier, B. Maro, and M.H. Verlhac. 2002. Meiotic spindle stability depends on MAPK-interacting and spindle-stabilizing protein (MISS), a new MAPK substrate. *J. Cell Biol.* 157:603–613.

Nigg, E.A. 2001. Mitotic kinases as regulators of cell division and its checkpoints. *Nat. Rev. Mol. Cell Biol.* 2:21–32.

Ray, L.B., and T.W. Sturgill. 1987. Rapid stimulation by insulin of a serine/threonine kinase in 3T3-L1 adipocytes that phosphorylates microtubule-associated protein 2 in vitro. *Proc. Natl. Acad. Sci. USA.* 84:1502–1506.

Reszka, A.A., R. Seger, C.D. Diltz, E.G. Krebs, and E.H. Fischer. 1995. Association of mitogen-activated protein kinase with the microtubule cytoskeleton. *Proc. Natl. Acad. Sci. USA.* 92:8881–8885.

Roberts, E.C., P.S. Shapiro, T.S. Nahreini, G. Pages, J. Pouyssegur, and N.G. Ahn. 2002. Distinct cell cycle timing requirements for extracellular signal-regulated kinase and phosphoinositide 3-kinase signaling pathways in somatic cell mitosis. *Mol. Cell. Biol.* 22:7226–7241.

Saxton, W.M., D.L. Stemple, R.J. Leslie, E.D. Salmon, M. Zavortink, and J.R. McIntosh. 1984. Tubulin dynamics in cultured mammalian cells. *J. Cell Biol.* 99:2175–2186.

Schwab, M.S., B.T. Roberts, S.D. Gross, B.J. Tunquist, F.E. Taieb, A.L. Lewellyn, and J.L. Maller. 2001. Bub1 is activated by the protein kinase p90 Rsk during Xenopus oocyte maturation. *Curr. Biol.* 11:141–150.

Shapiro, P.S., E. Vaisberg, A.J. Hunt, N.S. Tolwinski, A.M. Whalen, J.R. McIntosh, and N.G. Ahn. 1998. Activation of the MKK/ERK pathway during somatic cell mitosis: direct interactions of active ERK with kinetochores and regulation of the mitotic 3F3/2 phosphoantigen. *J. Cell Biol.* 142:1533–1545.

Solomon, M.J., M. Glotzer, T.H. Lee, M. Philippe, and M.W. Kirschner. 1990. Cyclin activation of p34cdc2. *Cell.* 63:1013–1024.

Spector, D.L., R.D. Goldman, and L.A. Lienhund. 1998. Cells A Laboratory Manual. Cold Spring Harbor Laboratory Press, Cold Spring Harbor, NY.

Verlhac, M.H., J.Z. Kubiak, M. Weber, G. Geraud, W.H. Colledge, M.J. Evans, and B. Maro. 1996. Mos is required for MAP kinase activation and is involved in microtubule organization during meiotic maturation in the mouse. *Development.* 122:815–822.

Walczak, C.E. 2001. Ran hits the ground running. *Nat. Cell Biol.* 3:E69–E70.

Wittmann, T., A. Hyman, and A. Desai. 2001. The spindle: a dynamic assembly of microtubules and motors. *Nat. Cell Biol.* 3:E28–E34.

Wright, J.H., E. Munar, D.R. Jameson, P.R. Andreassen, R.L. Margolis, R. Seger, and E.G. Krebs. 1999. Mitogen-activated protein kinase kinase activity is required for the G(2)/M transition of the cell cycle in mammalian fibroblasts. *Proc. Natl. Acad. Sci. USA.* 96:11335–11340.

Zecevic, M., A.D. Catling, S.T. Eblen, L. Renzi, J.C. Hittle, T.J. Yen, G.J. Gorbsky, and M.J. Weber. 1998. Active MAP kinase in mitosis: localization at kinetochores and association with the motor protein CENP-E. *J. Cell Biol.* 142:1547–1558.